

Electrodeposition of Advanced SPR Thin Film for Ischemia Modified Albumin Levels Determination and Potential Hypertension Diagnosis

Xinghui Zhou^{1#}, Zhaoqun Xiao^{2#}, Jianjun Lin^{3*}, Danping Wang², Xinhua Wang¹, Weixing Ji¹, Yao Zheng¹, Haiming Jin¹, Yan Zhang¹

¹ Department of examination, Taizhou Hospital of traditional Chinese and Western medicine, Taizhou 317523, China

² Department of Cardiology, Taizhou Hospital of traditional Chinese and Western medicine, Taizhou 317523, China

³ Department of Examination, Ningbo Fourth Hospital, Ningbo 315700, China

These authors contributed equally to this work

* E-mail: jianjun_lin@foxmail.com

Received: 24 November 2016 / Accepted: 3 March 2017 / Published: 12 July 2017

In this work, a novel silver dendrite sensor, which was an enhancement based on the mixed self-assembled monolayers, was studied and employed to fabricate a surface plasmon resonance (SPR) immunosensor for the detection of ischemia modified albumin (IMA). The limit of the IMA detection was enhanced to 4.7 ng/L by the proposed silver dendrite, in comparison with the direct binding SPR measurement. Besides, no interferent was recognized, which could result in the false positive outcomes. These results indicated that a facile method without label could be supplied by the SPR biosensor with remarkable properties to improve the sensitivity of the assay for the further diagnose of hypertension.

Keywords: Biosensor; Surface plasmon resonance; Ischemia modified albumin; Hypertension; Silver dendrites

1. INTRODUCTION

Primarily hypertension or cryptogenic hypertension, which is hazardous factor for inducing cardiovascular diseases, generally occupied above 90% of the diagnosed cases of hypertension [1]. Besides, it is recognized as an early sign of atherosclerosis and endothelial dysfunction, connecting with subclinical vascular impairment [2]. Numerous mechanisms have been proposed for the causation hypertension in the past years, including the endothelin system, the vasopressin system, the

vasoconstrictive mechanisms and the reactive oxygen species which has been reported recently during the development of human or experimental hypertension [3]. Moreover, the increased vascular oxidative stress is considered as the primary risk factor for the cardiovascular disease, as it could be related to the etiopathogenesis of hypertension [4]. The oxidation of lipoproteins and lipids, which are the oxidized low-density lipoprotein (Ox-LDL), is one of most significant processes [5]. In particular, Ox-LDL, which plays a significant role in etiopathogenesis of hypertension [6], is a primary factor to induce atherosclerosis and vessel wall injury [7]. Thus, to increase the Ox-LDL level in the atherosclerotic plaques is essential for the development of atherosclerosis. Besides, it is also in relation with atherogenesis through causing the cell proliferation and foam cell generation of the smooth muscle [8]. Both LDL and other serum lipids are under oxidative stress [10], where High density lipoprotein (HDL) becomes one of the most predominant and independent protective factors for the arteriosclerosis, which underlies the coronary heart disease [9].

However, a novel albumin modified with ischemia (IMA) has been reported recently, which is recognized as effective for detecting the severe myocardial ischemia. In 1990, IMA was first discovered and further confirmed in 1992 as the increased level of IMA in unstable angina and severe myocardial infarction was observed. Especially, in 2003, Food and Drug Administration in the United States approved this result [10]. The circulating albumin molecules are modified when ischemia presents and are independent on the cell death [11]. Albumin contains the N-terminal residues for binding metal, which could be modified through the oxidation with free radicals formed during ischemia via the depletion or acetylation of one or more amino acids residues, resulting in the low capacity to bind cobalt [12]. Thus, cobalt has been considered as an indicator for the assay, where the free cobalt atoms are incubated in the serum of patient. The modified albumin becomes incapable to bind cobalt when ischemia increases. Hence, the content of the free cobalt is in relation to the degree of the modified albumin generation. During the ischemia process, the damage is determined by the free radicals. Owing to the simple, rapid and low-cost measurement, IMA assay is promising, where 82% of the patients with unstable angina or alleged severe coronary syndrome [13]. Besides, IMA test is also potential in cardiac detection as the negative IMA result could classify the patients into the low-risk category through the original evaluation with the clinical presentation. Consequently, IMA research causes a significant cost saving.

SPR is an optical sensor for detecting the differences in the refractive index of the materials on the gold surface [14], which exhibits various advantages such as rapid analysis, real-time detection like in-situ or on-site and label-free assays [15], compared to the other approaches [16]. Due to these significant properties, massive efforts have been made in the SPR biosensors for developing the specific biomolecular binding, including the protein (enzymes, antigens and antibodies) interactions [17, 18], the virus recognition [19] and the hybridization of nucleic acid and protein [20, 21]. According to the previous research, the SPR technique could detect proteins in the level of 100 ng/L [22], where the sensitive is insufficient for the measurements of some specimens. The colloidal gold nanoparticles, which exhibited distinct advantages including the rapid and facile synthesis [23], narrow size distribution, adequate surface modification and the desirable biocompatibility, have been extensively employed in the analytical signal amplification as a label [24, 25]. Herein, a novel SPR

biosensor to determine IMA was constructed through assembling anti-IMA on the electrodeposited film of Ag NPs.

2. EXPERIMENTS

Immobilization of Anti-IMA: First, the ITO side was immersed in the solution of 11-mercaptopundecanoic acid (MUA) with a concentration of 0.01 M for 24 h at room temperature to generate the self-assembled monolayer (SAM). For the mixed SAM (mSAM), the gold side was modified with the mixture of 16-mercaptohexadecanoic acid (MHA) and 11-mercaptopundecanol (MUOH) in a ratio of 1:9 (v/v). Then, the obtained chip was rinsed with ethanol and ultrapure water and subsequently dried with nitrogen, where the stable and completely covered SAMs on the surface were obtained. Thereafter, the gold side was further dipped into the solution for 30 min, which was prepared by mixing N-hydroxysuccinimide (NHS, 0.1 M) and EDC (0.1 M) in a ratio of 1:1 (v/v). Then, anti-IMA was immobilized onto the surface in PBS (pH 7.4) with various concentrations for 1 h. Finally, the chip was immersed into the solution of ethanolamine (pH 8.5) with a concentration of 1 M for 20 min to deactivate the unreacted esters.

Electrodeposition of Ag NPs: The electrolyte solution was composed of sodium citrate ($C_6H_5O_7Na_3$, 0.2 mM), KNO_3 (0.1 M) and $AgNO_3$ (0.05 mM). The hierarchical Ag nanomaterials were immobilized on the surface of ITO glass modified with anti-IMA at -0.2 V for 3700 s, where the temperature was 27 °C. An electrochemical workstation was employed to perform the electrodeposition with a three electrode system. The ITO glass modified with anti-IMA was used as the working electrode, where the Pt plate and Ag/AgCl (3M) acted as the counter electrode and reference electrode, respectively. In this work, the potentials were related to SCE. The saturated solution of potassium nitrate, which was used to inhibit the pollution of chloride ion from the Ag/AgCl, was connected through a salt bridge filled with potassium nitrate and agar.

SPR Assays for IMA: First, various IMA solutions with a concentration of 0 to 100 µg/L in PBS buffer were used to rinse the ITO modified with anti-IMA/Ag NPs for 20 min with a rate of 10 mL/min, where the unbound was removed with PBS. Subsequently, the substrate was reformed through the injection of the mixture of NaOH (0.1 M) and SDS (0.05%) for 8 min every time in the presence of IMA with other concentration. The signal enhancement was also carried out with IMA/Ag NPs through a sequential injection process which was similar with the procedure described above.

The scanning electron microscopy (SEM, ZEISS X-MAX) was used to study the morphology and microstructure of the surface coatings. The XRD spectra of the coated pipe was obtained in the range of 20° to 80° in 2θ by XRD (PW3040/60 X'pert PRO). UV-vis spectrophotometer (Perkin Elmer Lambda 950) was employed for optical analysis.

3. RESULTS AND DISCUSSION

The sample, which was composed of the hierarchical Ag nanomaterials in high yield, was shown in Figure 1A. The as-deposited Ag with a hierarchical nanostructure, which seems to grow from

one point, was clearly illustrated in Figure 1B. Besides, it was also obvious that the diameter of the bottom structure was thinner compared to the upside. Here, the hierarchical nanostructure was considered approximately as a sphere in order to simplify the statistics of the size of the nanostructure. The relative standard deviation of the product size for 100 nanostructures was calculated to be 17.51%. A significant contrast was observed in our results compared with the Ag nanomaterials exhibiting large size distribution, which was synthesized through the electrodeposition with high precursor concentration as well as the reduction of Ag ions with Zn or Al plates [26-29]. Owing to the mild reduction of Ag ions with low precursor concentration, the uniformity of the nanostructure was improved. The large size distribution of the Ag nanostructures which was synthesized through electrodeposition was primarily caused by the gradual nucleation as well as the different growth rate at various growth phases at the constant potential. XPS patterns and EDS spectra illustrated in Figure 1C and 1D respectively confirmed the deposition of Ag.

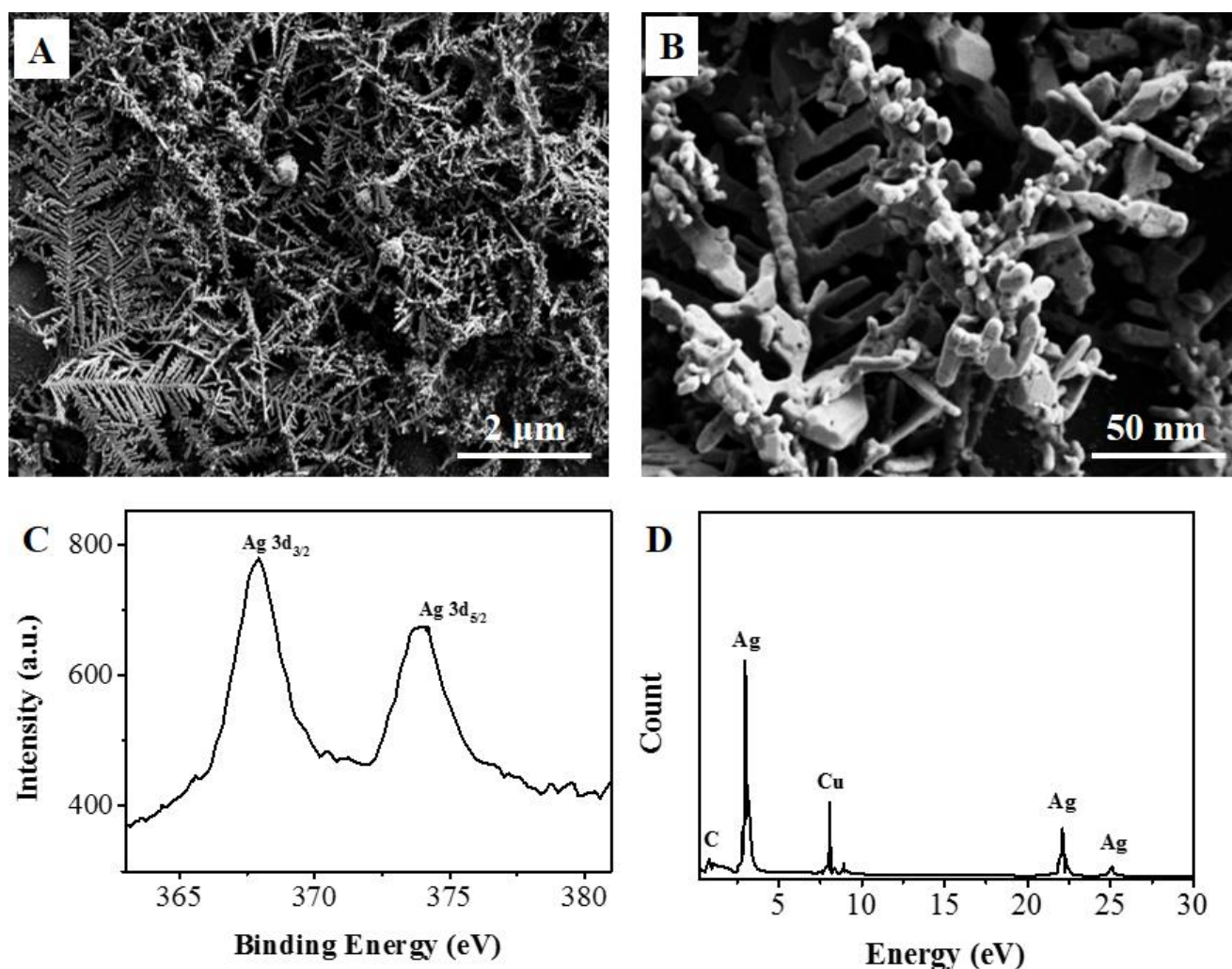


Figure 1. SEM images of the electrodeposited Ag nanomaterials with low magnification (A) and high magnification (B). XPS (C) patterns and EDS spectra (D) of the electrodeposited Ag nanomaterials.

The XRD patterns of the hierarchical Ag nanomaterials was clarified in Figure 2A. The peak at 36.50° indexed as the (111) plane is present with a high intensity, indicating that Ag deposits preferably as the (111) plane under these conditions. With an increasing proportion of AgNO_3 , peak growths are noticed at 42.67° , 62.92° , 75.90° and 79.83° , which are attributable to (200), (220), (311) and (222) silver face-centered-cube (fcc) crystal diffractions, respectively. An ultra-broad peak was observed in the UV-Vis spectrum of the hierarchical Ag nanostructure shown in Figure 3B, which was induced by the interparticle surface plasmon coupling effect [30-32]. Besides, the peak was also broadened by the size variation of the sample. The peaks present at 380 and 490 nm were attributed to the quadrupole and dipole plasmon resonance of Ag nanostructures, respectively [31, 33, 34]. In fact, the anisotropic nanoparticles exhibited the transverse and longitudinal characteristic adsorption bands.

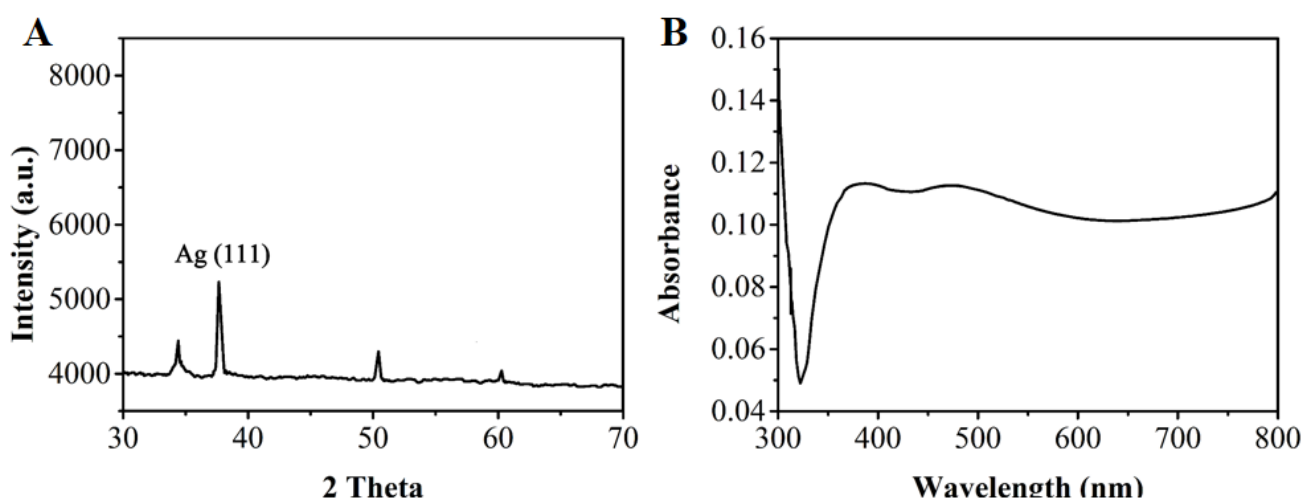


Figure 2. (A) XRD pattern of the hierarchical Ag nanostructures and (B) UV-vis absorption spectrum of the as-prepared sample.

SPR was an optoelectrical phenomenon, which was based on the electronic field on the surface of the sensor induced by plasmon. It was demonstrated that the distance between the silver sensing surface influenced the SPR response. A close relationship was observed between any SPR response and the tiny distance between the surface and the analyte. In this work, both MUA and the mixture of MHA and MUOH were investigated on the surface of ITO as a SAM. In Figure 3A, it was obvious that the monolayer of MUA exhibited a relatively low adsorption compared to the mixture, indicating that the mSAM displayed a higher signal enhancement. Hence, the mixture was selected to replace the carboxymethylated dextran, whereas the optimum ratio of MHA to MUOH was still under discussion. Thereafter, diverse mSAMs were prepared through the immersion of sensor into the solution of MHA and MUOH with various ratios. As shown in Figure 3B, the binding exhibited the highest SPR response when the ratio was set to be 3:7. The hydroxyl-terminated SAMs of MUOH reduced the non-specific binding and were employed to generate the chip surface as spacer, whereas the carboxyl-terminated SAMs of MHA were utilized to anchor IMA for immunoassays as the functional linkers. The phase segregation changed from order to disorder when increasing the length of the carbon

chain. There is evidence of plasmon resonance frequency shift only in the presence of both targets, indicating the very good selectivity of the artificial receptors here considered [35, 36]. The surface reactivity was enhanced by the formation of the rough surface by the Van der Waals attraction between the chains.

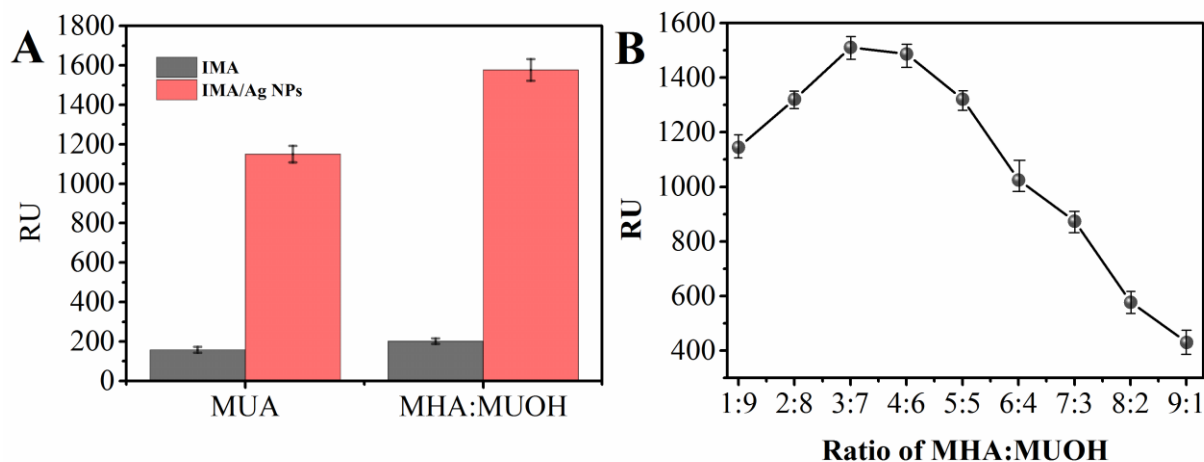


Figure 3. Effects of (A) the chips modified with the mixed self-assembled monolayer of MUA on IMA and IMA-Ag NPs (B) the varied ratio of MHA to MUOH from 1:9, 2:8, 3:7, 4:6, 5:5, 6:4, 7:3, 8:2 to 9:1.

In Figure 4A, it was obvious that the signal was enhanced remarkably by employing Ag NPs compared to the signal obtained in the absence of Ag NPs. Ag dendrites exhibited a soupier binding effect towards the antibody [37, 38]. The influence of IMA and Ag NPs with various ratios on the signal improvement was further studied. The results indicated that the signal enhancement was significantly determined by the size of the dendrites, which consisted of Ag NPs and the surrounding IMA molecules. The chances of the particles being bound to the surface could be increased by the proper ratios. In Figure 4B, the optimized ratio was selected to be 4:6 (v/v).

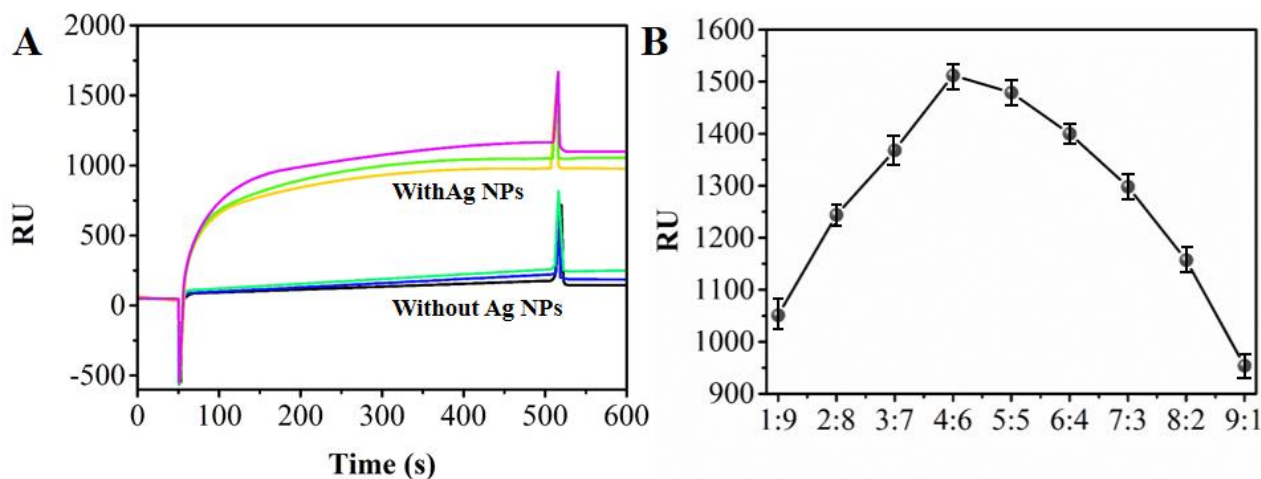


Figure 4. (A) The bioconjugation yield in sensograms for various approaches. (B) The influence of IMA and Ag NPs at various ratios obtained with SPR.

In the SPR sensing system, IMA was immobilized to the surface of the sensor modified with anti-IMA in prior to insert the mixture of IMA and Ag NPs. The analytical capacity of the proposed biosensor was analyzed through IMA with various concentrations. The distinct signals were observed through the insertion of two formats. Besides, the values of the signals were significantly in accordance with the enhancement theory with low and high concentrations. In Figure 5, it was obvious that the response signal increased when the concentration of IMA increased. In addition, the binding only cost 5 min without label through this method. Hence, the detection of the target was in real-time. The linear detection range of proposed method is from 0.1 to 50 $\mu\text{g/L}$. The limit of detection can be calculated to be 0.06 $\mu\text{g/L}$. Table 1 shows the comparison of our proposed IMA SPR sensor with some previously IMA determination reports.

Table 1. Comparison of proposed IMA SPR sensor with other IMA determination reports.

Method	LDR	LOD (μM)	Reference
Cobalt-albumin binding array	—	—	[39]
Quantum dot coupled X-ray fluorescence spectroscopy	0.08 to 8 $\mu\text{g/L}$	0.05 $\mu\text{g/L}$	[40]
Spectrophotometric determination	—	—	[41]
Polymerized crystalline colloidal array	0.2 to 1 $\mu\text{g/L}$	0.06 $\mu\text{g/L}$	[42]
Proposed SPR sensor	0.1 to 50 $\mu\text{g/L}$	0.06 $\mu\text{g/L}$	This work

In the case of direct assay, the limit of the detection with the sensor was found to be 100 ng/L. However, the binding performance obtained on the surface modified with anti-IMA suggested that the assay was enhanced significantly with Ag NPs. The concentration of anti-IMA was reduced to 4.7 ng/L from 100 ng/L through the signal enhancement compared to the traditional assay, which demonstrated that the limit of the detection was improved remarkably.

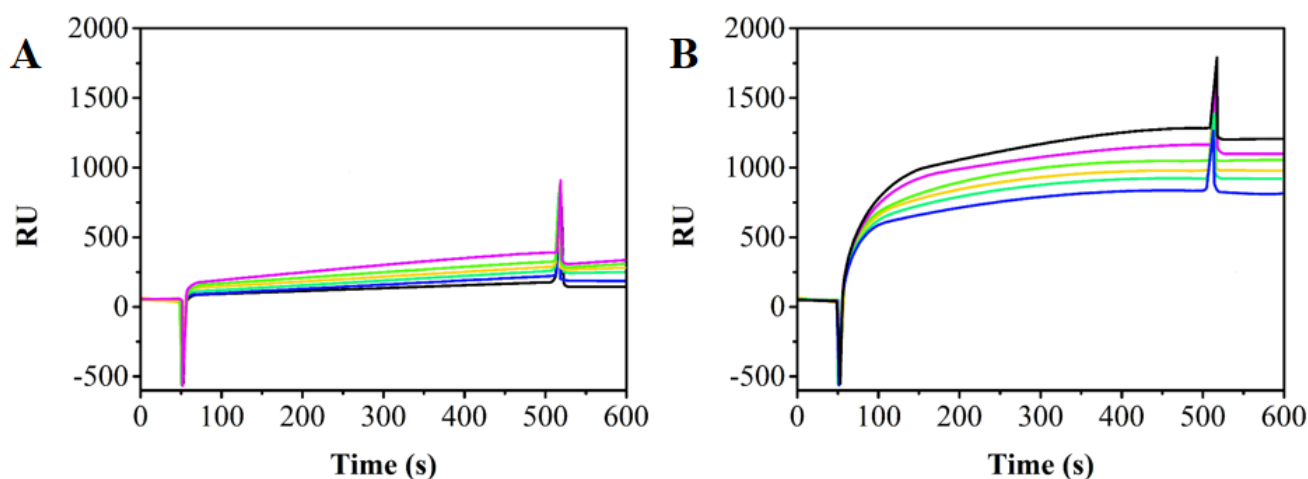


Figure 5. (A) The sensorgrams obtained with IMA in various concentrations in the absence of Ag NPs. (B) The sensorgrams obtained with IMA in diverse concentrations in the presence of Ag NPs. (concentration of the IMA: 0.1 $\mu\text{g/L}$, 0.5 $\mu\text{g/L}$, 1 $\mu\text{g/L}$, 10 $\mu\text{g/L}$, 50 $\mu\text{g/L}$)

Table 2. Selectivity of developed IMA biosensor.

Interfering Substance	Concentration (ng/L)	Δ RU	
		av ²	SD
Hep	200	6.9	7.01
Hb	200	6.7	8.51
Bil	200	9.3	3.66
TG	200	8.6	8.94
IMA(hypertension)	200	198.7	9.66
IMA(non- hypertension)	200	202.3	10.21

Furthermore, IMA exhibited a higher sensitivity and negative predictive value for the hypertension screening compared with traditional biochemical labels. However, a lower specificity was observed with IMA, in particular for the interferents such as bilirubin (Bil), hemoglobin (Hb), heparin (Hep) and triglyceride (TG). In this work, the pure IMA with definite concentration was employed to investigate whether IMA exhibited remarkably different between the hypertension and non-hypertension groups. As shown in Table 2, the sensor exhibited approximately same response signal towards those control groups. The surface modified with anti-IMA was immersed in the solution of Hep with a concentration of 200 ng/L in PBS buffer for 20 min, where Bil, Hb and TG were performed with the same process as Hep. The results indicated that no signal enhancement was observed, which meant this method exhibited outstanding selectivity.

In order to evaluate the capability of the developed sensor in the detection of IMA, the response behaviors of IMA with different real samples were examined. Five clinical serum samples containing IMA were examined using the proposed SPR sensor and the results were listed in Table 3. The relative errors of each method was calculated to be less than 7.71%. This reveals that the proposed SPR sensor is available for clinical analysis, and it serves an important alternative for hypertension diagnosis.

However, there are also disadvantages of SPR, as it cannot easily discriminate between specific and non-specific interactions with the sensor surface. Elaborate washing does not completely remove the non-specifically bound material; thus, reference material or control samples are needed to correct for the non-specific binding.

Table 3. Determination of IMA in clinical serum samples.

Sample	Added IMA (μ g/L)	Result (μ g/L)	RSD (%)
1	1	1.04	4.21
2	5	4.97	7.71
3	10	9.89	6.32
4	20	20.55	5.54
5	40	41.03	3.50

4. CONCLUSIONS

In summary, the potential of the SPR assay with high sensitivity for the determination of IMA was investigated through electrodepositing Ag NPs on the surface of ITO sensor. The proposed SPR

biosensor exhibited an outstanding performance towards the detection of IMA with low concentrations, where no interferent was observed which could cause false positive. Especially, the limit of detecting IMA with Ag NPs was improved to 4.7 ng/L. Thus, it was significantly component for the assay with patients, the blood albumin level of which was below 32 ng/L. An efficient method for the detection of IMA during the assay as well as further determination of hypertension could be supplied by the modified biosensor, which exhibited high sensitivity, outstanding signal response and remarkably low limit of detection.

References

1. A. Kumar, *Asian Pacific Journal of Tropical Disease*, 4 (2014) S429.
2. W. Abebe and M. Mozaffari, *Am J Cardiovasc Dis*, 1 (2011) 293.
3. A. Caballero, K. Santos, L. Osorio, V. Montagnani, G. Soodini, S. Porramatikul, O. Hamdy, A. Nobrega and E. Horton, *Diabetes Care*, 31 (2008) 576.
4. E. Grossman, *Diabetes Care*, 31 (2008) S185.
5. M. Assadpoor-Piranfar, A. Pordal and M. Beyranvand, *Arch Iran Med*, 12 (2009) 116.
6. G. Basati, M. Pourfarzam, A. Movahedian, S. Samsamshariat and N. Sarrafzadegan, *Clinics*, 66 (2011) 1129.
7. A. Gönenç, *Turk J Pharm Sci*, 9 (2012) 41.
8. B. Catagol and N. Ozen, *Curr Cardiol Rev*, 6 (2010) 309.
9. A. Kumar and U. Biswas, *Heart Asia*, 3 (2011) 115.
10. A. Wu, *MLO: Medical Laboratory Observer*, 35 (2003) 36.
11. R. Christenson, S. Duh, W. Sanhai, A.H. Wu, V. Holtman, P. Painter, E. Branham, F. Apple, M. Murakami and D. Morris, *Clinical Chemistry*, 47 (2001) 464.
12. D. Bar-Or, E. Lau, N. Rao, N. Bampos, J. Winkler and C. Curtis, *Annals of Emergency Medicine*, 34 (1999) S56.
13. D. Bar-Or, E. Lau and J. Winkler, *The Journal of Emergency Medicine*, 19 (2000) 311.
14. S. Roh, T. Chung and B. Lee, *Sensors*, 11 (2011) 1565.
15. E. Mauriz, A. Calle, J. Manclus, A. Montoya and L. Lechuga, *Anal Bioanal Chem*, 387 (2007) 1449.
16. T. Holford, F. Davis and S. Higson, *Biosensors and Bioelectronics*, 34 (2012) 12.
17. C. Fong, M. Wong, W. Fong and M. Yang, *Anal. Chim. Acta.*, 456 (2002) 201.
18. H. Šířová, H. Vaisocherová, J. Štěpánek and J. Homola, *Biosensors and Bioelectronics*, 26 (2010) 1605.
19. J. Mitchell, Y. Wu, C. Cook and L. Main, *Analytical Biochemistry*, 343 (2005) 125.
20. Y. Li, X. Liu and Z. Lin, *Food Chemistry*, 132 (2012) 1549.
21. V. Hodnik and G. Anderluh, *Sensors*, 9 (2009) 1339.
22. X. Cao, Y. Ye and S. Liu, *Analytical Biochemistry*, 417 (2011) 1.
23. J. Yuan, R. Oliver, J. Li, J. Lee, M. Aguilar and Y. Wu, *Biosensors and Bioelectronics*, 23 (2007) 144.
24. C. Huang, G. Yao, R. Liang and J. Qiu, *Biosensors and Bioelectronics*, 50 (2013) 305.
25. E. Azzam, A. Abd El-aal, O. Shekhah, H. Arslan and C. Wöll, *Journal of Dispersion Science and Technology*, 35 (2014) 717.
26. A. Gutés, C. Carraro and R. Maboudian, *Journal of the American Chemical Society*, 132 (2010) 1476.
27. P. Brejna, U. Sahaym, M. Norton and P. Griffiths, *J Phys Chem C*, 115 (2011) 1444.
28. S. Tang, X. Meng, C. Wang and Z. Cao, *Mater. Chem. Phys.*, 114 (2009) 842.
29. C. Gu and T. Zhang, *Langmuir*, 24 (2008) 12010.

30. J. Bian, Z. Li, Z. Chen, X. Zhang, Q. Li, S. Jiang, J. He and G. Han, *Electrochimica Acta*, 67 (2012) 12.
31. J. Bian, Z. Li, Z. Chen, H. He, X. Zhang, X. Li and G. Han, *Appl. Surf. Sci.*, 258 (2011) 1831.
32. Y. Xia, P. Yang, Y. Sun, Y. Wu, B. Mayers, B. Gates, Y. Yin, F. Kim and H. Yan, *Adv. Mater.*, 15 (2003) 353.
33. J. Zhang, X. Li, X. Sun and Y. Li, *J Phys Chem B*, 109 (2005) 12544.
34. Y. Song and H. Elsayed-Ali, *Appl. Surf. Sci.*, 256 (2010) 5961.
35. N. Cennamo, G. D'Agostino, M. Pesavento and L. Zeni, *Sensors and Actuators B: Chemical*, 191 (2014) 529.
36. M. Benounis, N. Jaffrezic, C. Martelet, I. Dumazet-Bonnamour and R. Lamartine, *Materials Transactions*, 56 (2015) 539.
37. B. Zhao, Y. Lu, C. Zhang, Y. Fu, S. Moeendarbari, S. Shelke, Y. Liu and Y. Hao, *Appl. Surf. Sci.*, 387 (2016) 431.
38. C. O'Regan, X. Zhu, J. Zhong, U. Anand, J. Lu, H. Su and U. Mirsaidov, *Langmuir*, 32 (2016) 3601.
39. D. Bar-Or, E. Lau and J. Winkler, *The Journal of Emergency Medicine*, 19 (2000) 311.
40. Y. Luo, C. Wang, T. Jiang, B. Zhang, J. Huang, P. Liao and W. Fu, *Biosensors and Bioelectronics*, 51 (2014) 136.
41. K. Maneewong, T. Mekrungruangwong, S. Luangaram, T. Thongsri and S. Kumphune, *Indian Journal of Clinical Biochemistry*, 26 (2011) 389.
42. J. Baca, D. Finegold and S. Asher, *The Analyst*, 133 (2008) 385.

© 2017 The Authors. Published by ESG (www.electrochemsci.org). This article is an open access article distributed under the terms and conditions of the Creative Commons Attribution license (<http://creativecommons.org/licenses/by/4.0/>).